= 203 Hz, CH), 153.3 (s, Fe—C), 204.5 (s, Ni—CO), 234 (br, Fe—CO and μ-CO); IR (KBr) 1975, 1957, 1801 cm^{-1}; FD-MS *m/z* 536 (M$^+$). Anal. Calcd for $C_{20}H_{16}O_3FeNi_3$: C, 44.80; H, 2.98. Found: C, 44.54; H, 3.20.

A 1:2 reaction of 1 (301 mg, 1.49 mmol) and 5 (905 mg, 3.00 mmol) in heated benzene (16 mL, for 8 h at 65 °C) gave 7 (208 mg, 0.39 mmol, 28% isolated yield based on 1).

Interaction of Fp*—C≡C—H (1*) with $Cp_2Ni_2(CO)_2$ (5). A benzene solution (20 mL) of 1* (170 mg, 0.63 mmol) and 5 (191 mg, 0.63 mmol) was heated for 27 h at 60 °C. Evaporation of the volatiles, extraction with ether, and filtration through an alumina pad followed by crystallization from ether–hexanes gave 7* (98 mg, 0.22 mmol, 33% yield based on $Cp_2Ni_2(CO)_2$) as brown crystals. 7*: ^{1}H NMR (C_6D_6) δ 1.32 (15 H, s, Cp*Fe) 5.08 (10 H, s, CpNi × 2), 7.73 (1 H, s, C_2H); ^{13}C NMR (C_6D_6) δ 9.6 (q, ^1J = 128 Hz, C_5Me_5), 87.1 (d, ^1J = 175 Hz, CpNi), 95.6 (s, C_5Me_5), 117.3 (d, ^1J = 201 Hz, CH), 163.9 (d, ^2J = 14 Hz, Fe—C), 205.9 (s, Ni—CO), 236.2 (Fe—CO and μ-CO); IR (KBr) 1972, 1950, 1788 cm^{-1}; FD-MS *m/z* 606 (M$^+$). Anal. Calcd for $C_{25}H_{26}O_3FeNi_3$: C, 49.53; H, 4.29. Found: C, 49.11; H, 4.29.

Attempts To Isolate 6*. Reactions of 1* and 5 in <3:1 ratio gave only a very small amount of 6*. While a 4:1 reaction produced a 3:4 mixture of 6* and 7*, repeated recrystallization resulted in recovery of excess 1* and the evaporated residue of the final mother liquor contained only small amounts of 6* and 7*. Attempted separation by column chromatography (alumina and silica gel) resulted in decomposition.

Conversion of 6 into 7 by Treatment with $Ni(CO)_4$. ***Caution*:** Due to the extreme toxicity of $Ni(CO)_4$ all the manipulations should be carried out in a well-ventilated place.

A benzene solution (3 mL) of 6 (80 mg, 0.18 mmol) and $Ni(CO)_4$ (~30 μL, 0.23 mmol) was stirred overnight at ambient temperature. A small portion (0.1 mL) of the mixture was taken out and dried. Formation of a considerable amount of 7 was indicated by the bridging CO stretching vibration at 1800 cm^{-1}. Then the remaining solution was heated for 7 h at 50 °C. After evaporation of the volatiles, 7 was isolated from the residue as described above. Recrystallization gave 7 (66 mg, 0.12 mmol) in 70% yield.

Interaction of Fp*—C≡C—Fp* (2) with $Cp_2Ni_2(CO)_2$ (5). A benzene solution (25 mL) of 2 (500 mg, 0.97 mmol) and 5 (290 mg, 0.97 mmol) was heated at 55 °C for 2 days. After consumption of 2 was checked by TLC, the volatiles were removed under reduced pressure. Extraction with hexanes and filtration through a Celite pad followed by crystallization at −20 °C gave 10 (157 mg, 0.39 mmol, 40%) as yellow black crystals: ^{1}H NMR (C_6D_6) δ 1.43 (15 H, s, Cp*Fe) 5.37 (5 H, s, CpNi); ^{13}C NMR (C_6D_6) δ 9.0 (C_5Me_5), 93.9 (CpNi), 97.3 (C_5Me_5), 240 (br, CO); IR (KBr) 1986, 1787 cm^{-1}. Anal. Calcd for $C_{18}H_{20}O_3FeNi$: C, 54.22; H, 5.02. Found: C, 53.66; H, 5.19.

X-ray Crystallography of 6, 7, and 10. Single crystals of 6, 7, and 10 were obtained by recrystallization from ether–hexanes–toluene and ether–hexanes mixed-solvent systems, respectively, and mounted on glass fibers.

Diffraction measurements were made on a Rigaku AFC-5R (6 and 10) and AFC-5 (7) automated four-circle diffractometer by using graphite-monochromated Mo Kα radiation (λ = 0.710 59 Å). The unit cell was determined and refined by a least-squares method using 24 independent reflections with 19° < 2θ < 21° (6 and 10) and 15° < 2θ < 20° (7). Data were collected with ω–2θ scan technique. If $\sigma(F)/F$ was more than 0.1, a scan was repeated up to three times and the results were added to the first scan. Three standard reflections were monitored at every 150 (6 and 10) and 100 (7) measurements. Data processing of 6 and 10 was performed on a Micro Vax II computer by using the TEXSAN structure-solving program system, and data processing of 7 was performed on a FACOM A-70 computer by using the R-CRYSTAN data collection program system. Both systems were obtained from the Rigaku Corp., Tokyo, Japan. Neutral scattering factors were obtained from the standard sources.[15] In the reduction of data, Lorentz and polarization corrections and an empirical absorption correction (ψ scan) were made.

6 crystallized in an orthorhombic system, and 7 and 10 crystallized in monoclinic systems. The structures were solved by using the TEXSAN structure-solving program system. The positions of the metal atoms were located by the direct method (MITHRIL), and the structures were expanded by a combination of the direct method and Fourier synthesis (DIRDIF). For 6 and 7 all the non-hydrogen atoms were refined anisotropically. The hydrogen atoms except C_2H were located at the ideal positions and were not refined, and the position of the C_2H atom was refined with a fixed isotropic thermal parameter [B(H) = 1.2B(C)]. During the refinement of the structure of 10 it became apparent that there was disorder in the Cp part, which was refined isotropically by using a rigid η^5-C_5H_5 model (C–C = 1.40 Å; C–H = 0.95 Å). The occupancy factor of the two components was determined to be C14–18:C14A–18A = 0.648:0.352. The other non-hydrogen atoms were refined anisotropically, and the hydrogen atoms were located at the ideal positions and were not refined [B(H) = 1.2B(C)].

Acknowledgment. This research was financially supported by a Grant-in-Aid from the Ministry of Education, Science, and Culture of the Japanese Government.

Supplementary Material Available: Tables of positional and anisotropic thermal parameters and bond lengths and angles for 6, 7, and 10 (23 pages). Ordering information is given on any current masthead page.

OM920241I

---

[15] *International Tables for X-ray Crystallography*; Kynoch Press: Birmingham, U.K., 1975; Vol. 4.

Synthesis and Molecular Structure of $Fe_2(CO)_8[\mu\text{-}CuP(t\text{-}Bu)_3]_2$: A Distorted Fe_2Cu_2 Core with a Doubly $Cu(PR_3)$ Bridged Fe–Fe Single Bond

Haibin Deng, David W. Knoeppel, and Sheldon G. Shore*

Department of Chemistry, The Ohio State University, Columbus, Ohio 43210

Received February 5, 1992

Summary: Reported here are the synthesis and molecular structure of $Fe_2(CO)_8[\mu\text{-}CuP(t\text{-}Bu)_3]_2$, which contains an Fe_2Cu_2 butterfly metal core with the Fe–Fe single bond doubly bridged by two $CuP(t\text{-}Bu)_3$ fragments. The differences in the Fe–Cu bond distances (ca. 0.1 Å) and the deviation of the metal core from planarity (43.8°) can be attributed to the second-order Jahn–Teller effect and the steric effect imposed by the bulky $P(t\text{-}Bu)_3$ ligands. Crystal data for $Fe_2(CO)_8[\mu\text{-}CuP(t\text{-}Bu)_3]_2$: orthorhombic, space group $P2_12_12_1$, a = 8.881 (3) Å, b = 14.208 (3) Å, c = 31.114 (6) Å, Z = 4, and R = 0.027.

Recently we reported the syntheses and molecular structures of several group 8–group 11 mixed-metal complexes $M_2(CO)_8(\mu\text{-}CuPCy_3)_2$ (M = Fe, Ru; Cy = tricyclohexyl), $[PPh_4][Fe_2(CO)_8(\mu\text{-}CuPCy_3)]$, and $[PPh_4]_2\{[Fe_2(CO)_8]_2[\mu_4,\eta^2\text{-}Cu_2(Cy_2PCH_2CH_2PCy_2)]\}$.[1] The molecular structures of $M_2(CO)_8(\mu\text{-}CuPCy_3)_2$ (M = Fe, Ru) are without precedent in that the metal–metal *single* bond (Fe–Fe or Ru–Ru) is doubly bridged by two $Cu(PCy_3)$ fragments.[1] Two types of structural distortions from a symmetrical D_{2h} four-metal core were recognized in M_2-

---

[1] Deng, D.; Shore, S. G. *Organometallics* 1991, *10*, 3486.

Table I. Crystallographic Data for $Fe_2(CO)_8[\mu\text{-}CuP(t\text{-}Bu)_3]_2$

formula	$C_{32}H_{54}Cu_2Fe_2O_8P_2$
mol wt	867.50
space group	$P2_12_12_1$
a, Å	8.881 (3)
b, Å	14.208 (3)
c, Å	31.114 (6)
V, $Å^3$	3925.9
Z	4
D(calc), g cm^{-3}	1.468
cryst dimens, mm	0.25 × 0.35 × 0.35
temp, °C	−60
radiatn (λ, Å)	Mo Kα (0.710730)
abs coeff, cm^{-1}	19.196
transmissn coeff	0.907–0.970
2θ limits, deg	4–50
scan mode	ω–2θ
no. of reflns measd	3919
no. of unique rflns	3703
no. of unique rflns $>3\sigma(I)$	2877
no. of variables	415
R_F	0.027
R_{wF}	0.035
GOF	1.173

$(CO)_8(\mu\text{-}CuPCy_3)_2$ (M = Fe, Ru): (1) distortion of the M_2Cu_2 metal core from a rhombus to a parallelogram with two long peripheral edges and two short ones, thus reducing the symmetry from D_{2h} to C_{2h}, and (2) puckering of the M_2Cu_2 metal core along the M–M vector by about 30°, further lowering the symmetry of the metal core from C_{2h} to C_2.[1] The puckering of the four-metal core is believed to be largely due to steric effects, as potential energy surfaces for the change in interplanar angles of butterfly clusters are usually soft and depend critcally on the steric requirements of the ligands spanning the wingtip positions of the butterfly.[2] On the other hand, it is hard to distinguish between steric effects and electronic effects as the cause of the first type of distortion, i.e., asymmetrical bridging of the two $Cu(PCy_3)$ fragments. As far as the possible electronic effects are concerned, a qualitative explanation based on group-theoretical arguments has been proposed, which invoke the second-order Jahn–Teller effect[3] as the cause of this asymmetrical bridging.[1]

It is of interest to investigate the degree of metal core distortions with phosphine ligands of various bulkiness. Accordingly, syntheses and structural characterization of $Fe_2(CO)_8(\mu\text{-}CuPR_3)_2$ have been attempted with different phosphines.

Results and Discussion

In the synthesis of $Fe_2(CO)_8(\mu\text{-}CuPR_3)_2$ choices of phosphine ligands are critical, being dependent upon the steric characters of the ligands. Thus, $Fe_2(CO)_8(\mu\text{-}CuPR_3)_2$ could be isolated with $P(t\text{-}Bu)_3$ but not with $P(n\text{-}Bu)_3$. In the latter case copper metal and intractable materials are formed. The synthesis of $Fe_2(CO)_8[\mu\text{-}CuP(t\text{-}Bu)_3]_2$ was carried out according to eq 1.

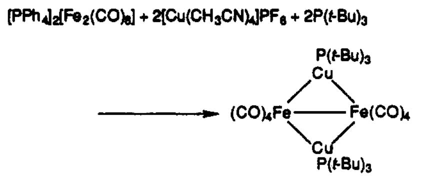

(1)

Table II. Positional Parameters and Their Estimated Standard Deviations for $Fe_2(CO)_8[\mu\text{-}CuP(t\text{-}Bu)_3]_2$

atom	*x*	*y*	*z*	*B*,[a] $Å^2$
Cu1	0.69652 (8)	0.99982 (4)	0.45331 (2)	2.26 (1)
Cu2	0.70636 (8)	1.09198 (4)	0.33330 (2)	2.28 (1)
Fe1	0.81542 (9)	0.96574 (5)	0.38042 (2)	1.89 (1)
Fe2	0.51336 (9)	1.02931 (6)	0.39105 (2)	2.08 (1)
P1	0.7274 (2)	1.0002 (1)	0.52514 (4)	1.85 (2)
P2	0.7567 (2)	1.2001 (1)	0.28209 (4)	2.17 (3)
O1	0.6889 (6)	0.8981 (3)	0.2991 (1)	3.71 (9)
O2	1.1202 (5)	0.9185 (4)	0.3538 (2)	5.8 (1)
O3	0.9302 (5)	1.1413 (3)	0.4179 (1)	3.9 (1)
O4	0.7912 (6)	0.7917 (3)	0.4303 (1)	4.5 (1)
O5	0.3624 (5)	1.0515 (4)	0.3081 (1)	4.2 (1)
O6	0.6063 (6)	1.2175 (3)	0.4194 (1)	4.2 (1)
O7	0.2425 (6)	1.0525 (4)	0.4420 (2)	6.0 (1)
O8	0.4648 (6)	0.8253 (3)	0.3993 (2)	5.7 (1)
C1	0.7348 (7)	0.9302 (4)	0.3306 (2)	2.5 (1)
C2	1.0009 (8)	0.9362 (4)	0.3646 (2)	3.6 (1)
C3	0.8796 (7)	1.0741 (4)	0.4039 (2)	2.5 (1)
C4	0.7963 (7)	0.8631 (4)	0.4131 (2)	2.9 (1)
C5	0.4337 (7)	1.0443 (4)	0.3387 (2)	2.9 (1)
C6	0.5785 (7)	1.1419 (4)	0.4085 (2)	2.8 (1)
C7	0.3504 (7)	1.0438 (5)	0.4221 (2)	3.6 (1)
C8	0.4920 (7)	0.9055 (5)	0.3960 (2)	3.3 (1)
C11	0.6667 (7)	1.1191 (4)	0.5475 (2)	2.8 (1)
C12	0.7387 (9)	1.1973 (4)	0.5198 (2)	3.8 (1)
C13	0.4962 (8)	1.1281 (5)	0.5416 (2)	4.1 (1)
C14	0.7080 (9)	1.1390 (5)	0.5943 (2)	3.9 (1)
C21	0.9301 (7)	0.9753 (4)	0.5421 (2)	2.7 (1)
C22	1.0252 (8)	1.0646 (5)	0.5340 (2)	4.0 (2)
C23	0.9965 (7)	0.8987 (5)	0.5126 (2)	3.6 (1)
C24	0.9511 (8)	0.9463 (5)	0.5889 (2)	3.9 (1)
C31	0.6000 (6)	0.9049 (4)	0.5481 (2)	2.6 (1)
C32	0.4567 (7)	0.9042 (4)	0.5215 (2)	3.4 (1)
C33	0.6719 (7)	0.8070 (4)	0.5416 (2)	3.4 (1)
C34	0.5603 (8)	0.9160 (5)	0.5968 (2)	3.9 (2)
C41	0.6913 (8)	1.3215 (4)	0.3005 (2)	3.4 (1)
C42	0.692 (1)	1.3982 (5)	0.2647 (2)	4.9 (2)
C43	0.789 (1)	1.3553 (5)	0.3377 (2)	4.9 (2)
C44	0.5298 (9)	1.3123 (5)	0.3179 (2)	4.6 (2)
C51	0.9702 (7)	1.2023 (5)	0.2734 (2)	3.3 (1)
C52	1.0319 (8)	1.2894 (5)	0.2502 (2)	5.0 (2)
C53	1.0486 (8)	1.1963 (5)	0.3173 (2)	4.2 (2)
C54	1.0195 (9)	1.1140 (6)	0.2499 (2)	4.8 (2)
C61	0.6637 (8)	1.1703 (5)	0.2281 (2)	3.5 (1)
C62	0.4954 (8)	1.1930 (5)	0.2297 (2)	5.0 (2)
C63	0.731 (1)	1.2209 (5)	0.1895 (2)	5.4 (2)
C64	0.674 (1)	1.0628 (5)	0.2213 (2)	4.8 (2)

[a] Anisotropically refined atoms are given in the form of the isotropic equivalent displacement parameter, defined as $^4/_3[a^2(\beta(1,1)) + b^2(\beta(2,2)) + c^2(\beta(3,3)) + ab(\cos\gamma)(\beta(1,2)) + ac(\cos\beta)(\beta(1,3)) + bc(\cos\alpha)(\beta(2,3))]$.

The molecular structure of $Fe_2(CO)_8[\mu\text{-}CuP(t\text{-}Bu)_3]_2$ was determined with single-crystal X-ray diffraction data. Figure 1 shows two views of the molecular structure; crystal data, positional parameters, and bond distances and angles are given in Tables I–III, respectively.

As in $M_2(CO)_8(\mu\text{-}CuPCy_3)_2$ (M = Fe, Ru), two $Cu(P(t\text{-}Bu)_3$ fragments bridge the Fe–Fe single bond in the title compound, forming a so-called butterfly structure. The Fe–Fe bond distance of 2.850 (1) Å is comparable with that in $Fe_2(CO)_8(\mu\text{-}CuPCy_3)_2$ (2.862 (1) Å).[1] Deviation of the metal core Fe_2Cu_2 in the title compound from planarity is 43.8°, significantly larger than deviations in $M_2(CO)_8(\mu\text{-}CuPCy_3)_2$ (31.7° for M = Fe and 28.3° for M = Ru). Bulkier phosphine ligands apparently cause greater deviation of the metal core from planarity (cone angles are as follows:[4] $P(t\text{-}Bu)_3$, 182°, PCy_3, 170°). The difference of deviations from planarity between $Fe_2(CO)_8[\mu\text{-}CuP(t\text{-}Bu)_3]_2$ and $Fe_2(CO)_8(\mu\text{-}CuPCy_3)_2$ and the difference of cone angles between $P(t\text{-}Bu)_3$ and PCy_3 are both 12°, which is

---

(2) Mingos, D. M. P.; May, A. S. In The *Chemistry of Metal Cluster complexes*; Shriver, D. F., Kaesz, H. D., Adams, R. D., Eds.; VCH: New York, 1990; p 31.

(3) Cotton, F. A.; Fang, A. *J. Am. Chem. Soc.* **1982**, *104*, 113.

(4) Tolman, C. A. *Chem. Rev.* **1977**, *77*, 313.

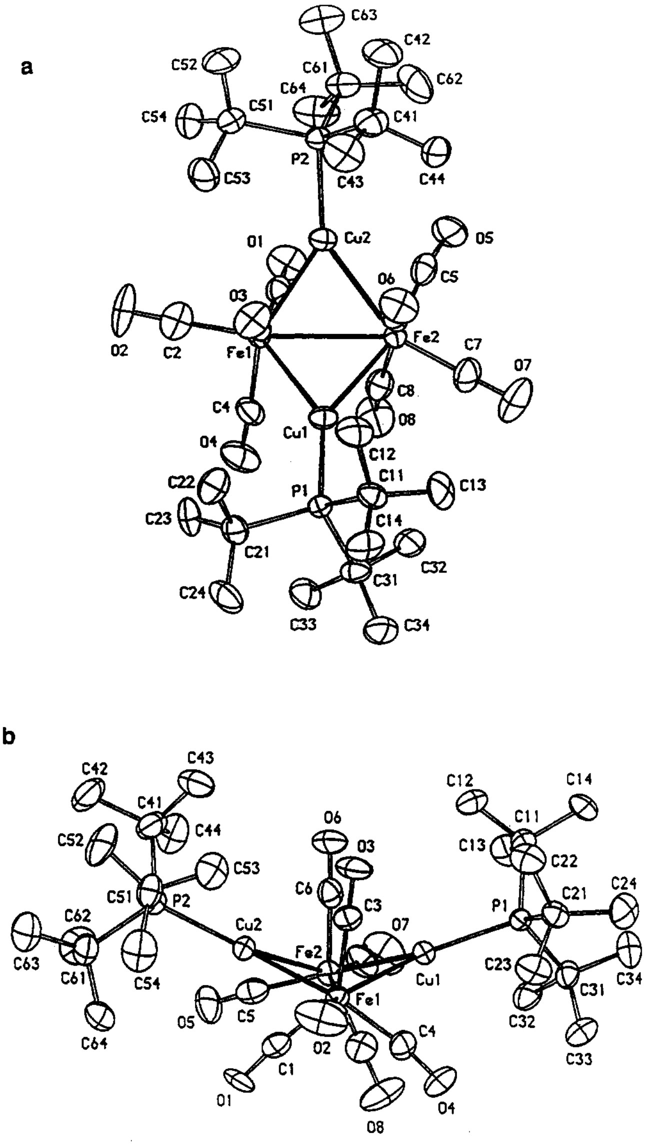

Figure 1. Two different views (top, a; bottom, b) of the molecular structure of $Fe_2(CO)_8[\mu\text{-}CuP(t\text{-}Bu)_3]_2$ showing the thermal ellipsoids at the 30% probability level. Hydrogen atoms are omitted.

probably coincidental. The smaller deviation of the M_2Cu_2 core from planarity in $Ru_2(CO)_8(\mu\text{-}CuPCy_3)_2$ compared to that in $Fe_2(CO)_8(\mu\text{-}CuPCy_3)_2$ (the difference being 3.3°) can be attributed to the longer metal–metal bonds in the former complex, which reduce steric strains.

Table III. Selected Bond Distances (Å) and Angles (deg) for $Fe_2(CO)_8[\mu\text{-}CuP(t\text{-}Bu)_3]_2$

	Distances		
Cu1–Fe1	2.548 (1)	P1–C11	1.905 (5)
Cu1–Fe2	2.564 (1)	P1–C21	1.909 (6)
Cu1–P1	2.252 (1)	P1–C31	1.903 (6)
Cu2–Fe1	2.511 (1)	P2–C41	1.907 (6)
Cu2–Fe2	2.638 (1)	P2–C51	1.915 (6)
Cu2–P2	2.258 (1)	P2–C61	1.918 (6)
Fe1–Fe2	2.850 (1)	O1–C1	1.157 (6)
Fe1–C1	1.780 (6)	O2–C2	1.140 (7)
Fe1–C2	1.769 (7)	O3–C3	1.141 (7)
Fe1–C3	1.797 (6)	O4–C4	1.147 (7)
Fe1–C4	1.786 (6)	O5–C5	1.148 (7)
Fe2–C5	1.790 (6)	O6–C6	1.153 (7)
Fe2–C6	1.785 (7)	O7–C7	1.148 (7)
Fe2–C7	1.751 (6)	O8–C8	1.168 (8)
Fe2–C8	1.777 (7)		
	Angles		
Fe1–Cu1–Fe2	67.76 (3)	Cu2–Fe2–C5	66.2 (2)
Fe1–Cu1–P1	146.45 (5)	Cu2–Fe2–C6	72.2 (2)
Fe2–Cu1–P1	145.77 (5)	Cu2–Fe2–C7	150.7 (2)
Fe1–Cu2–Fe2	67.16 (3)	Cu2–Fe2–C8	117.6 (2)
Fe1–Cu2–P2	145.24 (5)	Fe1–Fe2–C5	107.7 (2)
Fe2–Cu2–P2	147.03 (5)	Fe1–Fe2–C6	90.8 (2)
Cu1–Fe1–Cu2	102.95 (3)	Fe1–Fe2–C7	151.5 (2)
Cu1–Fe1–Fe2	56.39 (3)	Fe1–Fe2–C8	78.3 (2)
Cu1–Fe1–C1	131.5 (2)	C5–Fe2–C6	107.4 (3)
Cu1–Fe1–C2	132.7 (2)	C5–Fe2–C7	99.3 (3)
Cu1–Fe1–C3	66.9 (2)	C5–Fe2–C8	98.9 (3)
Cu1–Fe1–C4	67.0 (2)	C6–Fe2–C7	89.7 (3)
Cu2–Fe1–Fe2	58.55 (3)	C6–Fe2–C8	153.6 (3)
Cu2–Fe1–C1	62.6 (2)	C7–Fe2–C8	88.9 (3)
Cu2–Fe1–C2	111.5 (2)	Cu1–P1–C11	109.3 (2)
Cu2–Fe1–C3	75.4 (2)	Cu1–P1–C21	112.9 (2)
Cu2–Fe1–C4	151.5 (2)	Cu1–P1–C31	107.4 (2)
Fe2–Fe1–C1	79.2 (2)	C11–P1–C21	109.3 (3)
Fe2–Fe1–C2	169.6 (2)	C11–P1–C31	109.0 (3)
Fe2–Fe1–C3	88.8 (2)	C21–P1–C31	109.0 (3)
Fe2–Fe1–C4	95.9 (2)	Cu2–P2–C41	110.1 (2)
C1–Fe1–C2	93.7 (3)	Cu2–P2–C51	107.8 (2)
C1–Fe1–C3	136.4 (2)	Cu2–P2–C61	112.4 (2)
C1–Fe1–C4	103.0 (3)	C41–P2–C51	109.2 (3)
C2–Fe1–C3	91.2 (3)	C41–P2–C61	109.3 (3)
C2–Fe1–C4	93.0 (3)	C51–P2–C61	107.8 (3)
C3–Fe1–C4	119.9 (3)	Fe1–C1–O1	172.9 (5)
Cu1–Fe2–Cu2	99.07 (3)	Fe1–C2–O2	178.5 (7)
Cu1–Fe2–Fe1	55.85 (3)	Fe1–C3–O3	175.2 (5)
Cu1–Fe2–C5	163.4 (2)	Fe1–C4–O4	172.2 (5)
Cu1–Fe2–C6	73.2 (2)	Fe2–C5–O5	169.8 (5)
Cu1–Fe2–C7	97.3 (2)	Fe2–C6–O6	173.3 (6)
Cu1–Fe2–C8	80.8 (2)	Fe2–C7–O7	179.0 (6)
Cu2–Fe2–Fe1	54.29 (3)	Fe2–C8–O8	174.2 (6)

The approximate C_2 symmetry observed in the molecular structures of $M_2(CO)_8(\mu\text{-}CuPCy_3)_2$ (M = Fe, Ru) does not exist in that of the title compound, and the coordination geometry around each Fe atom in the title compound is irregular. The four Fe–Cu bond distances are as follows: Cu1–Fe1 = 2.548 (1) Å; Cu1–Fe2 = 2.564 (1) Å; Cu2–Fe1 = 2.511 (1) Å; Cu2–Fe2 = 2.638 (1) Å. The difference in the Cu2–Fe1 and Cu2–Fe2 bond distances is more than 0.1 Å, although the distortion does not follow the same pattern as in $M_2(CO)_8(\mu\text{-}CuPCy_3)_2$ (M = Fe, Ru).[1] As pointed out above, the two factors which are believed to determine metal core distortions are the second-order Jahn–Teller effect, which would cause the reduction of the point symmetry of the planar metal core from D_{2h} to C_{2h}, and a steric contribution from phosphine ligands, which would cause the puckering of the metal core. In the case of $M_2(CO)_8(\mu\text{-}CuPCy_3)_2$ (M = Fe, Ru) the *pseudo*-C_2 axis is retained in the puckered core.[1] In the present example the symmetry of the core is further reduced to C_1 due to increased steric effects of the $P(t\text{-}Bu)_3$ ligands. Specifically, two factors may be in effect: steric repulsion between the $P(t\text{-}Bu)_3$ ligands and the carbonyls of the $Fe(CO)_4$ groups, and crystal packing forces exerted on the $Fe_2(CO)_8[\mu\text{-}CuP(t\text{-}Bu)_3]_2$ molecules. However, energetically unfavorable short intra- and intermolecular contacts (<3 Å) were not observed; presumably they have been avoided due to the structural distortions of the $Fe_2(CO)_8[\mu\text{-}CuP(t\text{-}Bu)_3]_2$ molecules.

In solution, the $Fe_2(CO)_8[\mu\text{-}CuP(t\text{-}Bu)_3]_2$ molecule is stereochemically nonrigid, as its ^{13}C and ^{31}P NMR spectra show only a single resonance from room temperature down to −80 °C.

As in $M_2(CO)_8(\mu\text{-}CuPCy_3)_2$ (M = Fe, Ru), short Cu⋯C contact distances are observed in the title compound: Cu1⋯C3 = 2.47 Å; Cu1⋯C4 = 2.47 Å; Cu1⋯C6 = 2.67 Å; Cu1⋯C8 = 2.88 Å; Cu2⋯C1 = 2.31 Å; Cu2⋯C3 = 2.69 Å; Cu2⋯C5 = 2.52 Å; Cu2⋯C6 = 2.70 Å. We have suggested in our previous paper that weak infrared absorptions at 1720–1740 cm^{-1} might be due to short Cu⋯C contacts in the solid-state structures.[1] While the infrared spectra of the single crystals of $M_2(CO)_8(\mu\text{-}CuPCy_3)_2$ (M = Fe, Ru) in Nujol mulls do not show any absorptions in the bridging carbonyl region, the infrared spectrum of the title compound as well as those of $[PPh_4][Fe_2(CO)_8(\mu\text{-}CuPCy_3)]$ and $[PPh_4]_2\{[Fe_2(CO)_8]_2[\mu_4,\eta^2\text{-}Cu_2(Cy_2PCH_2CH_2PCy_2)]\}$ show broad weak absorptions at 1736, 1734, and 1720 cm^{-1}, respectively, although there are no bridging carbonyls in the solid-state structures.[1] Considering that the shortest Cu⋯C contacts are 2.39 Å in $Fe_2(CO)_8(\mu\text{-}CuPCy_3)_2$, 2.58 Å in $Ru_2(CO)_8(\mu\text{-}CuPCy_3)_2$, 2.31 Å in $[PPh_4][Fe_2(CO)_8(\mu\text{-}CuPCy_3)]$, 2.21 Å in $[PPh_4]_2\{[Fe_2(CO)_8]_2[\mu_4,^2\text{-}Cu_2(Cy_2PCH_2CH_2PCy_2)]\}$, and 2.31 Å in the title compound, it seems that a weak absorption will result at 1720–1740 cm^{-1} if the Cu–C contact distances fall below the threshold value of ca. 2.3 Å.

Experimental Section

All manipulations were carried out on a standard high-vacuum line or in a drybox under an atmosphere of dry, pure N_2. CH_3CN was dried over P_4O_{10} with continuous stirring for 2–3 days followed by distillation into storage bulbs. Toluene was dried over sodium and was distilled prior to use. Hexane was stirred over concentrated H_2SO_4 for 2–3 days followed by extraction with distilled water and then dried over CaH_2 and sodium. $P(t\text{-}Bu)_3$ (Strem Chemicals) was used as received. $[Cu(CH_3CN)_4][PF_6]$[5] and $[PPh_4]_2[Fe_2(CO)_8]$[6] were prepared by procedures reported in the literature.

IR spectra were recorded with 2-cm^{-1} resolution using a Mattson-Polaris FT-IR spectrometer. Solution spectra were obtained in Perkin-Elmer liquid cells with 0.5-mm Teflon spacers and KBr windows. Proton NMR (δ(TMS) 0.00 ppm), ^{31}P NMR (δ(85% H_3PO_4) 0.00 ppm), and ^{13}C NMR (δ(TMS) 0.00 ppm) spectra were obtained on a Bruker AM-250 NMR spectrometer operating at 250.14, 101.25, and 62.90 MHz, respectively. Elemental analyses were performed by Oneida Research Services, Whitesboro, NY.

Preparation of $Fe_2(CO)_8[\mu\text{-}CuP(t\text{-}Bu)_3]_2$. In the drybox, 80 mg (0.395 mmol) of $P(t\text{-}Bu)_3$ and 147 mg (0.394 mmol) of $[Cu(CH_3CN)_4][PF_6]$ were dissolved in 15 mL of dry CH_3CN in a flask; 5 mL of CH_3CN solution containing 210 mg (0.207 mmol) of $[PPh_4]_2[Fe_2(CO)_8]$ was added dropwise to the former mixture while it was stirred. The solution turned green immediately, and a mixture of dark green and white precipitates formed. After all the $[PPh_4]_2[Fe_2(CO)_8]$ was added, the flask was connected to a vacuum line extractor and brought out of the drybox. The solution was stirred for another 15 min, and CH_3CN was then removed under vacuum. A 15-mL amount of dry toluene was condensed into the flask at −78 °C. The product was dissolved in toluene, and the solution was filtered, leaving white $[PPh_4][PF_6]$ on the glass frit. The solvent was pumped away, and the collection flask was connected to a fresh extractor in the drybox. A minimal amount of CH_3CN was condensed into the flask at −78 °C, and the solid was washed again with CH_3CN and filtered. The product was collected on the frit and dried under vacuum: yield 110 mg, 64%.

The same synthetic procedure was carried out with $P(n\text{-}Bu)_3$. Instead of $Fe_2(CO)_8[\mu\text{-}CuP(n\text{-}Bu)_3]_2$, copper metal and intractable materials were formed.

Anal. Calcd for $C_{32}H_{54}Cu_2Fe_2O_8P_2$: C, 44.31; H, 6.27. Found: C, 44.33; H, 6.13. IR (THF; ν_{CO}, cm^{-1}): 2029 (w), 1986 (s), 1926 (s). IR (crystals in Nujol mull; ν_{CO}, cm^{-1}): 2030 (w), 1986 (s), 1979 (s, sh), 1952 (m), 1924 (s), 1906 (s), 1889 (m), 1872 (m), 1720 (w, br). ^1H NMR ($CDCl_3$, 303K; δ (ppm)): 1.50 (d, $^3J_{PH}$ = 12 Hz). $^{31}P\{^1H\}$ NMR ($CDCl_3$, 303 K; δ (ppm)): 58.22 (s). $^{13}C\{^1H\}$ NMR ($CDCl_3$, 303 K; δ (ppm)): 213.90 (s, CO), 36.93 ($1J_{PC}$ = 7.5 Hz), 32.01 (d, $^2J_{Pc}$ = 6.0 Hz).

X-ray Crystal Structure Determination. Single crystals of $Fe_2(CO)_8[\mu\text{-}CuP(t\text{-}Bu)_3]_2$ (green) were grown by keeping a saturated hexane solution of $Fe_2(CO)_8[\mu\text{-}CuP(t\text{-}Bu)_3]_2$ at −40 °C for 2 days. Crystals of suitable size were mounted under N_2 in glass capillaries. All crystallographic data were collected on an Enraf-Nonius CAD4 diffractometer with graphite-monochromated Mo Kα radiation. Unit cell parameters were obtained by a least-squares refinement of the angular settings from 25 reflections, well distributed in reciprocal space and lying in a 2θ range of 24–30°. Crystallographic data are given in Table I. The diffraction symmetry (D_{2h}, $2/m2/m2/m$) and the systematic absences ($h00$ for $h = 2n + 1$; $0k0$ for $k = 2n + 1$; $00l$ for $l = 2n + 1$) uniquely determine the space group $P2_12_12_1$ (No. 19).

The data were corrected for Lorentz and polarization effects, decay, and absorption (empirically from ψ-scan data). The structure was solved by employing a combination of MULTAN 11/82 and difference Fourier techniques with analytical scattering factors used throughout the structure refinement and both real and imaginary components of the anomalous dispersion included for all non-hydrogen atoms. All the crystallographic computations were carried out on a DEC Vax station 3100 computer, using the Structure Determination Package (SDP).[7] After all of the non-hydrogen atoms were located and refined, one hydrogen atom for each methyl group was located from difference Fourier maps and the remaining hydrogen atoms were placed at calculated positions (C–H = 0.95 Å, B(H) = 1.3[B(C)]Å^2). Then with the positional and thermal parameters of all of the hydrogens fixed, the non-hydrogen atoms were refined anisotropically. New hydrogen positions were calculated again, and this procedure was repeated until the parameters of non-hydrogen atoms were refined to convergence (final shift/error ≤0.03). The highest residual peak on the final difference Fourier map is 0.52 e/Å^3.

The least-squares refinements were performed on two enantiomorphic models related by the inversion center. They resulted in two sets of R, Rw, and GOF values: 0.035, 0.046, 1.554 and 0.027, 0.035, 1.173, respectively. The bond distances and angles for the two models are essentially the same. The structure of the latter enantiomorphic model is reported in this note.

Acknowledgment. This work was supported by the National Science Foundation through Grant CHE91-04035. NMR spectra were obtained at the Ohio State University Campus Chemical Instrument Center, funded in part by NSF Grant 79-10019 and NIH Grant 1 S10 PRO140518-01A.

Supplementary Material Available: Listings of crystallographic data, positional parameters, calculated hydrogen atom positional parameters, anisotropic thermal parameters, and bond distances and bond angles (8 pages). Ordering information is given on any current masthead page.

OM920064L

---

[5] Kubas, G. J. *Inorg. Synth.* **1979**, *19*, 90.

[6] Bhattacharyya, N. K.; Coffy, T. J.; Quintana, W.; Salupo, T. A.; Bricker, J. C.; Shay, T. B.; Payne, M.; Shore, S. G. *Organometallics* **1990**, *9*, 2368.

[7] SDP (developed by B. A. Frenz and Associates, Inc., College Station, TX 77840) was used to process X-ray data, to apply corrections, and to solve and refine the structures.